

## ORIGINAL ARTICLE

# Neurovascular coupling varies with level of global cerebral ischemia in a rat model

Wesley B Baker<sup>1</sup>, Zhenghui Sun<sup>2,3</sup>, Teruyuki Hiraki<sup>2</sup>, Mary E Putt<sup>4</sup>, Turgut Durduran<sup>5</sup>, Martin Reivich<sup>2</sup>, Arjun G Yodh<sup>1</sup> and Joel H Greenberg<sup>2</sup>

In this study, cerebral blood flow, oxygenation, metabolic, and electrical functional responses to forepaw stimulation were monitored in rats at different levels of global cerebral ischemia from mild to severe. Laser speckle contrast imaging and optical imaging of intrinsic signals were used to measure changes in blood flow and oxygenation, respectively, along with a compartmental model to calculate changes in oxygen metabolism from these measured changes. To characterize the electrical response to functional stimulation, we measured somatosensory evoked potentials (SEPs). Global graded ischemia was induced through unilateral carotid artery occlusion, bilateral carotid artery occlusion, bilateral carotid and right subclavian artery (SCA) occlusion, or carotid and SCA occlusion with negative lower body pressure. We found that the amplitude of the functional metabolic response remained tightly coupled to the amplitude of the SEP at all levels of ischemia observed. However, as the level of ischemia became more severe, the flow response was more strongly attenuated than the electrical response, suggesting that global ischemia was associated with an uncoupling between the functional flow and electrical responses.

*Journal of Cerebral Blood Flow & Metabolism* advance online publication, 3 October 2012; doi:10.1038/jcbfm.2012.137

**Keywords:** cerebral hemodynamics; evoked potentials; global ischemia; intrinsic optical imaging; neurovascular coupling

## INTRODUCTION

In healthy brains, localized increases in neuronal activity are strongly correlated, both spatially and temporally, with localized increases in cerebral blood flow (CBF) and cerebral metabolic consumption of oxygen (CMRO<sub>2</sub>).<sup>1</sup> Thus, quantification of hemodynamics because of increased neuronal activity, i.e., neurovascular coupling, has long been a topic of intense interest. In addition to being critical for the interpretation of techniques such as functional magnetic resonance imaging that use hemodynamic responses to map brain function, neurovascular coupling also has a role in several diseases, including Alzheimer's disease<sup>2</sup> and cerebral ischemia.<sup>3</sup> In this study, the effects of global cerebral ischemia on neurovascular coupling in a rat animal model are investigated.

Specifically, functional CBF, CMRO<sub>2</sub>, oxy-hemoglobin concentration (HbO), deoxy-hemoglobin concentration (HbR), and total hemoglobin concentration (HbT) responses to forepaw stimulation on rats were measured at several levels of global ischemia from very mild (CBF ~90% of normal supply) to more severe (CBF ~40% of normal supply). The combined optical techniques of laser speckle contrast imaging<sup>4,5</sup> and optical imaging of intrinsic signals<sup>6,7</sup> were used to make these measurements. To characterize neuronal activity, the electrical somatosensory evoked potentials (SEP) were also collected simultaneously with the optical hemodynamic measurements. To our knowledge, this is the first study that examines functional activation during graded ischemia.

This study is also motivated by the notion that functional stimulation can be used as a treatment for stroke.<sup>8,9</sup> Fox and Raichle<sup>10</sup> first reported that localized CBF increases caused by functional stimulation vastly exceed the localized CMRO<sub>2</sub> increases in healthy humans. This observation suggests that the oxygen delivery increase to the tissue from functional stimulation exceeds the oxygen consumption increase.<sup>11</sup> If the mismatch between the CBF response (surrogate for oxygen delivery) and CMRO<sub>2</sub> response persists during ischemia, then repeated application of functional stimulation during ischemia could increase the base level of oxygen in the brain.

For more significant ischemia (e.g., CBF supply below 40% of normal levels), no hemodynamic response to functional stimulation was observed. For less severe ischemic tissue, however, both hemodynamic and electrical responses to stimulation were present. In this paper, we will show that at these ischemic levels, CMRO<sub>2</sub> and SEP functional responses remained tightly coupled. Importantly, we discovered that as the animals became ischemic, the CBF response was more strongly attenuated than the CMRO<sub>2</sub> response. This observation suggests that, at least in *global* ischemia, oxygen delivery and consumption increases caused by stimulation become more balanced with ischemic severity. If the same is true in *focal* ischemia, then the mechanism for the neuroprotection of functional stimulation during ischemia reported in the literature<sup>8,9</sup> is probably not related to CBF changes. However, the potential for activation of collateral blood flow through leptomeningeal anastomoses during functional stimulation in focal ischemia necessitates that similar data be

<sup>1</sup>Department of Physics and Astronomy, University of Pennsylvania, Philadelphia, Pennsylvania, USA; <sup>2</sup>Department of Neurology, University of Pennsylvania, Philadelphia, Pennsylvania, USA; <sup>3</sup>Department of Neurosurgery of General Hospital of PLA, Beijing, China; <sup>4</sup>Department of Biostatistics and Epidemiology, University of Pennsylvania, Philadelphia, Pennsylvania, USA and <sup>5</sup>ICFO-Institut de Ciències Fotoniques, Mediterranean Technology Park, Castelldefels (Barcelona), Spain. Correspondence: WB Baker, Department of Physics and Astronomy, University of Pennsylvania, 2095 33rd Street, Philadelphia, PA 19104, USA. E-mail: wbaker@sas.upenn.edu or wbb5uva@gmail.com

This work is supported by the National Institutes of Health grants R01-NS057400 and R01-NS060653 as well as award P30-HD026979 (Intellectual and Developmental Disabilities Research Center) from the Eunice Kennedy Shriver National Institute of Child Health and Human Development.

Received 19 April 2012; revised 17 August 2012; accepted 23 August 2012

collected in focal ischemia models. The results in the present paper also support the notion that in healthy tissue, oxygen delivery increases from functional stimulation exceed oxygen consumption increases.<sup>11,12</sup> If the oxygen delivery and consumption increases were in balance, then the expectation is the CBF and CMRO<sub>2</sub> responses would be attenuated at the same rate by ischemia, which was not observed.

## MATERIALS AND METHODS

### Surgical Preparation

All procedures were in accordance with guidelines established by the National Institutes of Health and approved by the Institutional Animal Care and Use Committee of the University of Pennsylvania (approval #801100). Adult male Sprague-Dawley rats ( $N=46$ ,  $327 \pm 31$  g; Charles River, Wilmington, MA, USA) were anesthetized with 4% isoflurane in a bell jar, intubated, and then mechanically ventilated with 1.5% isoflurane in a mixture of oxygen and nitrous oxide (3:7). End-tidal CO<sub>2</sub> was monitored and the ventilation rate was adjusted to maintain an arterial CO<sub>2</sub> pressure close to 40 mmHg. Polyethylene catheters were placed in the femoral artery for blood pressure monitoring and the femoral vein for drug administration. Throughout the study, body temperature was measured with a rectal probe and maintained at  $37.5 \pm 0.2^\circ\text{C}$  with a heating pad (ATC1000, World Precision Instruments, Sarasota, FL, USA). In preparation for hemodynamic imaging, the rats were secured in a stereotaxic head holder. After reflecting their scalps, their skulls were uniformly thinned to translucency over a 5-by-5 mm window encompassing the right forepaw area of the cerebral cortex (center  $\sim 3.5$  mm directly lateral to bregma) (i.e., black square in Figure 1A) with a dental drill. To reduce specular reflections, ultrasound gel was applied to the translucent thinned skull and a glass coverslip placed on top. As depicted in Figure 1A, two 1 mm burr holes were drilled through the skull down to the dura ( $\sim 3.5$  mm lateral and 3 mm anterior of bregma;  $\sim 2.5$  mm directly posterior to lambda) for the placement of electrodes to measure the SEPs resulting from forepaw stimulation.

To induce global ischemia, animals were held in a supine position while a midline neck incision was made. Both common carotid arteries (CCA) were isolated from the surrounding connective tissue, and loose snares made from a polyethylene catheter (PE-10, Clay Adams, Parsippany, NJ, USA) were carefully placed around them for later remote occlusion. To achieve more severe ischemia, a partial sternotomy was also performed in the last 39 animals in the study. After separating sterno-hyoid muscle, the bifurcation of the right CCA and the right subclavian artery (SCA) from the aorta was carefully dissected and exposed. A snare was then placed around the right SCA between the first and second bifurcation of the right SCA. Finally, to even further increase the degree of ischemia, the lower bodies of the last 17 animals in the study were placed inside a custom-made pressure chamber after the snares were in position. The pressure chamber applied negative pressure to the rats, causing blood to pool in the lower part of the body.<sup>13</sup> The snares were tightened and negative pressure was applied sequentially to create different levels of cerebral ischemia from mild to severe.

For functional stimulation, two needle electrodes were inserted subdermally in the left forepaw of each rat, contra-lateral to the translucent imaging window. After the surgical preparation,  $\alpha$ -chloralose (60 mg/kg) was administered intravenously and the isoflurane was discontinued. Nitrous oxide was also discontinued and replaced with nitrogen gas. Anesthesia was maintained with an intravenous infusion of  $\alpha$ -chloralose (30 mg/kg per hour). On completion of the study, animals were euthanized with an overdose of barbiturate.

A control group ( $N=5$ ) was prepared in the same manner as described above with loose snares placed around both carotid arteries and the right SCA. However, these snares were not tightened to cause ischemia.

### Experiment Protocol

Figure 2 is a timeline of the study. As described above, the aim of the experiment was to create different levels of global ischemia and to measure the hemodynamic and electrical responses to forepaw stimulation. We generated different levels of ischemia by right common carotid artery occlusion (RCCAO), bilateral common carotid artery occlusion (RCCAO + LCCAO), bilateral common carotid artery occlusion with right SCA occlusion (RCCAO + LCCAO + RSCAO), and three vessel occlusion with lower body negative pressure applied in a pressure chamber. After

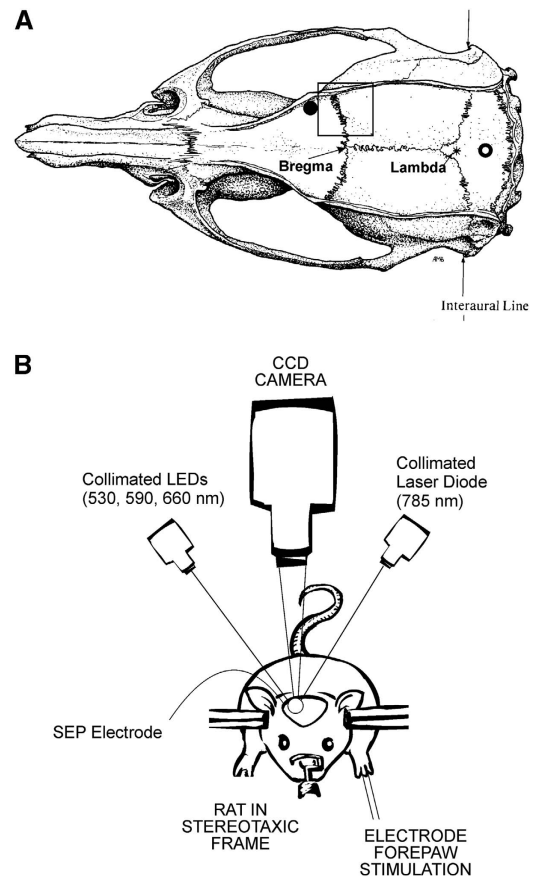


**Figure 1.** (A) Diagram of the rat brain showing the  $5 \times 5$  mm thinned part of the skull over the forepaw area of the cerebral cortex for hemodynamic imaging (black square) and the burr hole locations for electrodes to measure somatosensory evoked potentials (SEPs) (filled and open circles). (B) Schematic of instrument used for optical imaging of hemodynamics.

inducing each condition of ischemia, we waited 5 minutes to allow flow to stabilize before starting functional stimulation. The control group of animals shared the same timeline except that we did not occlude any arteries or apply lower body negative pressure. After euthanizing the animals, laser speckle images were collected for 5 minutes to obtain a biological zero correction to the CBF measurements.<sup>14</sup>

The forepaw stimulation paradigm, which was executed during the time windows marked DA (i.e., data acquisition) in Figure 2, consisted of a train of constant current rectangular pulses (amplitude 1.5 mA, duration 300  $\mu\text{s}$ ) delivered to the forepaw at 3 Hz for 4 seconds by a commercial high voltage stimulus isolator (A360; World Precision Instruments). The stimulation train was repeated every 30 seconds for a total time period of 8 minutes. After letting the animal rest for 4 minutes with no stimulation, the stimulation trains were resumed every 30 seconds for another 8 minutes. During these 8 minute periods, laser speckle and spectral images were collected sequentially for hemodynamic imaging, and electrical SEPs were recorded. This stimulation paradigm was repeated for every level of ischemia, as indicated in Figure 2. Five minutes before the first data acquisition, blood was withdrawn from the femoral artery for blood gas analysis.

### Optical Instrument

To obtain images of changes in blood flow and oxygenation, the techniques of laser speckle contrast imaging and optical imaging of intrinsic signals were combined.<sup>6</sup> As depicted in Figure 1B, a 60-mm lens (Apo-Componon 2.8/40; Schneider-Kreuznach, Bad Kreuznach, Germany) was used to form an image of the 5-by-5 mm forepaw region of the cerebral cortex on a 12-bit TEC cooled CCD camera (UP-680CL-12B, Uniq Vision Inc., Santa Clara, CA, USA) with unity magnification. Interleaved

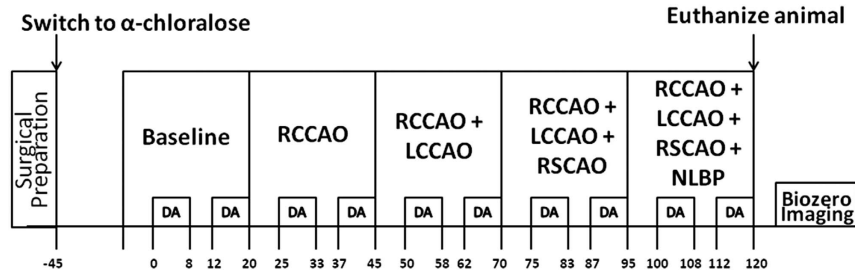


**Figure 2.** Schematic showing the timeline of the study in minutes (time axis not to scale). DA stands for data acquisition, where we collected laser speckle and spectral images and applied forepaw stimulation trains (1.5 mA, 0.3 ms rectangular pulses delivered at 3 Hz for 4 seconds) every 30 seconds as described in the text. The top row of boxes indicates the cerebral blood flow (CBF) conditions, which are baseline (i.e., preischemic), right common carotid artery occlusion (RCCAO), right and left common carotid artery occlusion (RCCAO + LCCAO), right and left common carotid artery occlusion with right subclavian artery occlusion (RCCAO + LCCAO + RSCAO), and the occlusion of the previous three arteries with the application of the negative lower body pressure (NLBP).

images (exposure time  $T = 4$  ms) under different illumination sources were then captured and recorded using a frame grabber (Grablink Avenue, Euresys Inc., San Juan Capistrano, CA, USA) and imaging software (StreamPix, NorPix, Montreal, QC, Canada).

The illumination source used for laser speckle contrast imaging of CBF was a collimated 785 nm laser diode (Sanyo, DL7140-2015, 785 nm, 70 mW; Thorlabs, Newton, NJ, USA) mounted on a temperature-controlled heat sink (LDM21 Laser Diode Temperature Controlled Mount; Thorlabs) and driven by a commercial driver (LDC 500 Laser Diode Controller; Thorlabs). The illumination sources used for optical imaging of intrinsic signals to measure changes in HbO and HbR were three collimated light emitting diodes (LEDs) mounted on heat sinks with central wavelengths of 530, 590, and 660 nm (M530L2-C1, M590L2-C1, M660L2-C1; Thorlabs) driven by commercial drivers (LEDD1B T-Cube LED Driver; Thorlabs).

Commercial software (SciWorks; DataWave Technologies, Boulder, CO, USA) was used to program pulse sequences of digital outputs from an A/D board (DataWave Technologies) to control the timing for the interleaved imaging. With this instrument, we acquired three spectral images and four speckle images per second.

### Somatosensory Evoked Potential Recordings

To measure the SEP response to stimulation, a 1-mm diameter silver/silver chloride ball electrode and a reference silver screw electrode were placed on the dura in the burr holes indicated by the filled and open black circles in Figure 1A, respectively. The recording electrodes were connected to a low-impedance HS4 headstage (World Precision Instruments), which amplified and digitized the voltage difference between the two electrodes before sending the signal to a Digital BioAmp (DB4; World Precision Instruments), where the signal was further amplified and filtered between 5 and 500 Hz.

### Optical Image Analysis

Laser speckle contrast imaging of CBF has been discussed extensively in previous publications,<sup>4</sup> and the specific analysis used in this study to calculate CBF from speckle contrast images is described by Zhou *et al.*<sup>14</sup> It was assumed that the static scattering contribution to the speckle contrast signal from the thinned skull<sup>15</sup> was negligible, since we saw very similar flow responses to studies where the skull was completely removed.<sup>16</sup> Since we were interested in functional CBF responses to stimulation, the CBF images were averaged across stimulation trials for each level of ischemia.

Optical imaging of intrinsic signals (or spectral imaging) to determine HbO and HbR is also a well-established technique.<sup>17,18</sup> As with CBF, the intensity images of each LED were averaged across stimulation trials at each level of ischemia. The averaged spectral intensity images of the three LEDs were converted to images of HbO and HbR via a modified Beer-Lambert law (see Appendix).

We used a compartmental model to calculate CMRO<sub>2</sub> images from our measurements of CBF, HbO, and HbR.<sup>19</sup>

$$CMRO_2 = \frac{SaO_2}{\gamma SaO_2} \frac{HbO}{HbT} \times CBF \times [D_2]_a \quad (1)$$

Here, HbT is the measured total hemoglobin concentration (i.e.,  $HbT = HbO + HbR$ ),  $SaO_2$  is the oxygen saturation in the cerebral arterioles (taken

to be 1),  $\gamma$  is the blood volume fraction contained in the venous compartment of the vascular system, and  $[O_2]_a$  is the blood arteriolar oxygen concentration. There is mounting evidence that oxygen extraction takes place in arteries and arterioles, and as a result, the arterioles directly feeding the cerebral capillary beds may have a lower saturation than the systemic arterial saturation.<sup>20</sup> In the present study, all animals breathed 30% oxygen resulting in high systemic arterial oxygen tensions (~120 mm Hg). Thus, even with oxygen extraction in the arteries and a potential small pH shift in the capillary blood, the arteriolar saturation will still be close to one throughout the study.

Equation 1 is a steady-state model for CMRO<sub>2</sub>. To estimate the errors in this model when applying it to the dynamic situation of functional stimulation, we followed Vazquez's *et al.*<sup>12</sup> approach of applying a dynamic compartment model to solve for CMRO<sub>2</sub> using input measurements from our previous study of cerebral tissue oxygen tension and blood flow in healthy rats during functional stimulation.<sup>21</sup> The increases in CMRO<sub>2</sub> during functional activation computed with this dynamic model were then compared with the increases computed with the steady-state model (Equation 1). This comparison showed that the calculated peak increases in CMRO<sub>2</sub> due to stimulation for the dynamic and steady-state models were within 2% of each other. Consequently, in the present study we use the peak increase from functional stimulation to characterize the response.

Under the assumptions that  $SaO_2$ ,  $[O_2]_a$ , and  $\gamma$  remain constant over time, substituting measurements of HbO, HbR, and CBF into Equation 1 result in an index that is proportional to CMRO<sub>2</sub>. Although it is feasible that these assumptions may be violated during ischemia, our group and others have shown the calculated metabolic changes from Equation 1 to be relatively insensitive (i.e., <5%) to most of the likely physiological cases that violate these assumptions.<sup>19,22</sup>

### Quantifying Hemodynamic and Somatosensory Evoked Potential Responses to Stimulation

Figures 3A and 3B contain montages of fractional CBF and CMRO<sub>2</sub> responses to stimulation for an exemplar animal averaged across all trials during the CBF baseline period of Figure 2. To quantify the hemodynamic responses of CBF and CMRO<sub>2</sub>, as well as the hemoglobin concentrations HbO, HbR, and HbT (image montages not shown), we followed the same approach as Durduran *et al.*<sup>16</sup> to select a region of interest (ROI). *A priori* information about the stimulus paradigm was used by computing a temporal correlation coefficient at every image pixel between CBF and the forepaw stimulus<sup>16</sup> during the preischemic baseline period. To apply a consistent threshold across all animals for ROI selection, the resulting image of correlation coefficients was normalized by the maximum pixel, resulting in an image of normalized correlation coefficients scaled from 0 to 1 (Figure 3C). An ROI consisting of all pixels with normalized correlation coefficients above 0.8 was arbitrarily chosen, and hemodynamic temporal response curves at each level of ischemia were obtained by averaging over all pixels within the ROI. We note here that we did not observe significant changes in our results when we tried using different correlation coefficient thresholds of 0.9 or 0.7 for the ROI, indicating robustness to the particular ROI threshold.

At ischemic condition  $i$  in an animal (e.g.,  $i = RCCAO$ ,  $RCCAO + LCCAO$ ; see Figure 2), the hemodynamic responses were quantitatively

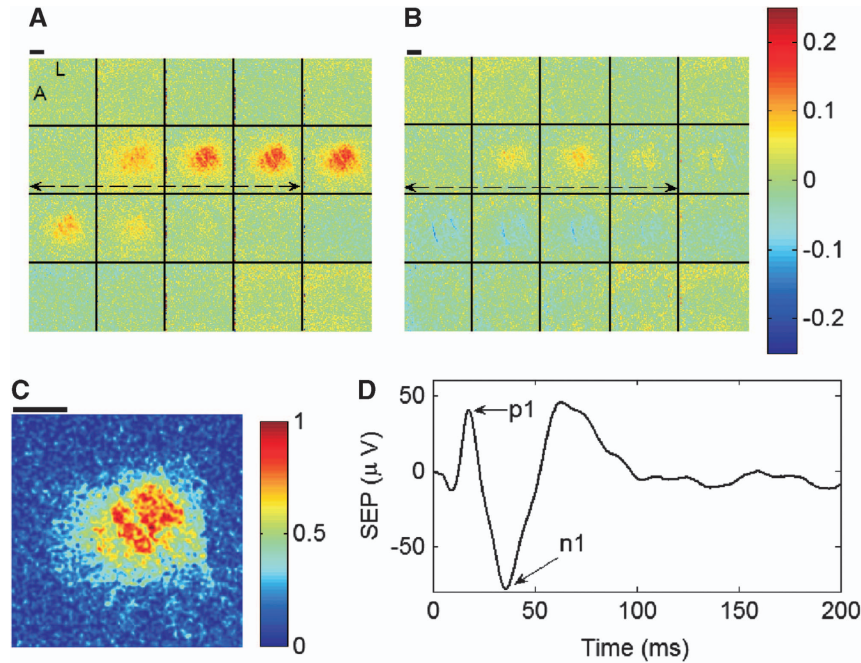


**Figure 3.** Image montages of fractional changes in cerebral blood flow (CBF) (A) and cerebral metabolic consumption of oxygen (CMRO<sub>2</sub>) (B) averaged across stimulation trials during the baseline, or preischemic, CBF condition for an exemplar animal. The fractional changes are relative to the mean of the parameters over the 5-second prestimulus time windows. Each image in the montages is spaced one second apart when read from left to right and top to bottom. The dashed double arrows indicate the 4-second forepaw stimulus, and the letters L and A within the first image of the CBF montage stand for lateral and anterior, respectively, to indicate image orientation. For region of interest (ROI) selection, a temporal correlation coefficient was computed at every pixel between CBF and the forepaw stimulus during preischemic stimulation, and the resulting correlation coefficient image was then normalized to the maximum pixel.<sup>16</sup> The ROI for the animal in this figure consists of all pixels in the animal's normalized correlation coefficient image (C) with values > 0.8 (see text). The thick black lines in (A) through (C) are 1 mm scale bars. (D) The somatosensory evoked potential (SEP) signal averaged across stimulation trials during the preischemic baseline condition of the same animal. The difference between the p1 and n1 peaks in the SEP signal was used to characterize the electrical response to stimulation.

characterized by their average peak increases from baseline because of stimulation, i.e.,  $\langle \Delta x \rangle_i = \langle x_{\text{peak}} - x_0 \rangle_i$ , where  $x$  refers to the CBF index, CMRO<sub>2</sub> index, HbO, HbR, or HbT. The SEP response, in turn, was characterized at condition  $i$  by the average difference between the  $p1$  and  $n1$  peaks of the signal (Figure 3D), which is denoted as  $\langle \Delta \text{SEP} \rangle_i$ . Ultimately, our interest is in how ischemia affects the relationship between the hemodynamic responses and the SEP response. To make the quantified responses unitless, which will facilitate comparison between the different response parameters at different ischemic levels, the hemodynamic and SEP responses at ischemic condition  $i$  were normalized by their preischemic baseline responses,  $\langle \Delta x \rangle_{\text{BL}}$  and  $\langle \Delta \text{SEP} \rangle_{\text{BL}}$ :

$$\text{Normalized hemodynamic response} = \langle \Delta x \rangle_i / \langle \Delta x \rangle_{\text{BL}} \quad (2a)$$

$$\text{Normalized SEP response} = \langle \Delta \text{SEP} \rangle_i / \langle \Delta \text{SEP} \rangle_{\text{BL}} \quad (2b)$$

The level of ischemia, or fraction of the normal CBF supply to the brain, reached because of the  $i$ th ischemic condition in an animal was determined quantitatively by averaging the prestimulus speckle CBF index during condition  $i$ ,  $\langle \text{CBF}_0 \rangle_i$ , and dividing this by the same average of CBF during the baseline condition,  $\langle \text{CBF}_0 \rangle_{\text{BL}}$ :

$$\text{CBF level} = \frac{\langle \text{CBF}_0 \rangle_i}{\langle \text{CBF}_0 \rangle_{\text{BL}}} \quad (3)$$

Also of interest is the affect of cerebral ischemia on SEP latency, which we define as the time after stimulus onset of the p1 peak in the SEP signal.

### Statistical Analysis

Across animals, the degree of ischemia attained after each of the manipulations was quite heterogeneous. Thus, although blood flow was decreased only through three artery occlusions and negative lower body

pressure, many different CBF levels ranging from very mild ischemia (i.e., 0.94) to severe ischemia (i.e., 0.36) were achieved in the animals. A major goal of this study was to determine whether there were differences in the mean CBF, CMRO<sub>2</sub>, and SEP normalized functional responses (Equations 2a and 2b) as a function of CBF level (Equation 3). To address this, a mixed effects model was used.<sup>23</sup> This procedure is conceptually similar to repeated measures ANOVA but allows the CBF level to be treated as a continuous variable. Initial graphical procedures suggested that in many cases the association between CBF level and the normalized functional responses was nonlinear. Thus, a natural cubic spline was used to model the mean CBF, CMRO<sub>2</sub>, and SEP normalized functional responses separately at each CBF level.

We additionally fit two natural cubic spline models to these three types of normalized responses (i.e., CBF, CMRO<sub>2</sub>, and SEP) simultaneously to determine the statistical significance of the differences in patterns over CBF level that we observed between these different types of responses. In one model, these differences were allowed to follow a parallel, albeit nonlinear pattern over CBF level. In the second model, the response types were allowed to change differently over CBF level. We applied a likelihood ratio test to these two models to test the null hypothesis that the three functional response types are all affected the same by CBF level. We also determined the significance of the differences between the SEP response and the other two response types by considering the Wald statistics for each of the terms in the spline of the second model. We then repeated this analysis to compare SEP responses with the HbO, HbR, and HbT responses as a function of CBF level.

The analysis described above addresses the global question of whether there were differences in the mean CBF, CMRO<sub>2</sub>, HbO, HbR, HbT, and SEP responses as a function of CBF level. Another important question is if there are differences, then what are the ranges of CBF levels where these responses are different. To address this, we used individual mixed effects models with a natural cubic spline to model the mean logarithms of the ratios of SEP response with the hemodynamic responses (i.e.,  $\log(\text{SEP}/\text{CBF})$ ,

log(SEP/HbO), and log(SEP/HbR)) as a function of CBF level. The hemodynamic responses were significantly different from SEP at CBF levels where the 95% CIs from these models did not overlap zero.

Finally, we used a mixed effects model to test the hypothesis that SEP latency increased with CBF level. As with the normalized responses, a natural cubic spline was used to model the mean SEP latency as a function of CBF level, and the overall significance was assessed using a likelihood ratio test.

These mixed effects models were implemented with library (nlme) and library (splines) in R 2.13.<sup>24</sup> A Type I error rate of 0.05 and 95% confidence intervals on the population mean (95% CI) were used.

## RESULTS

Before ischemia, the population means and standard deviations of pH, PaO<sub>2</sub>, and PaCO<sub>2</sub> determined from blood gas analysis were 7.44 ± 0.09, 124 ± 21, and 37 ± 8 mm Hg, respectively, and the arterial blood pressure was 106 ± 6 mm Hg. To aid the visualization of the effects of graded cerebral ischemia in this animal model on blood pressure, hemodynamic responses, and electrical responses, we discretized ischemic CBF levels (Equation 3) into bins of width 10 percentage points (i.e., 0.85 to 0.95, 0.75 to 0.85, ..., 0.35 to 0.45) and determined parameter averages across animals at CBF levels within these bins. The arterial blood pressures (mean ± SD) at these binned CBF levels were 115 ± 9, 122 ± 12, 112 ± 7, 118 ± 12, 117 ± 15, and 95 ± 19 mm Hg for the CBF levels of 0.85 to 0.95, 0.75 to 0.85, 0.65 to 0.75, 0.55 to 0.65, 0.45 to 0.55, and 0.35 to 0.45, respectively.

Figure 4 shows average fractional hemodynamic temporal response curves across animals at each binned CBF level of ischemia. Before ischemia (CBF Level 1 panel in Figure 4), CBF has the largest response of the hemodynamic parameters, with an average peak increase of 21%, while CMRO<sub>2</sub> peaked at 12%. HbO and HbR peaked at 8% and 8%, respectively, while a small 2% peak increase in HbT was observed. All the hemodynamic functional responses were attenuated as the animals became more ischemic, and once the CBF level reached 0.4, the responses essentially disappeared. Also, notice in Figure 4 that the peaks of the CBF and CMRO<sub>2</sub> responses approach each other as the level of ischemia increases, indicating that global ischemia more strongly attenuates the CBF response.

Corresponding to the average hemodynamic responses in Figure 4 are the average electrical SEP responses shown in Figure 5. As with the hemodynamic responses, the SEP response is attenuated as the level of ischemia increases. However, the SEP response has not vanished at the CBF level of 0.4, whereas the blood flow response is very much attenuated. Additionally, Figure 5 contains the mean SEP latency at each binned CBF level. The observed increase in SEP latency with ischemia relative to the preischemic latency is highly significant ( $P < 0.0001$ ).

Interestingly, the CBF response is attenuated more strongly at milder levels of global ischemia than the CMRO<sub>2</sub> and SEP responses (Figures 6 and 7). Figure 6 is a bar plot showing the mean normalized hemodynamic and SEP responses, as defined by Equations 2a and 2b, at each CBF level bin. Figure 6A suggests that the CMRO<sub>2</sub> response is tightly coupled to SEP as the animals

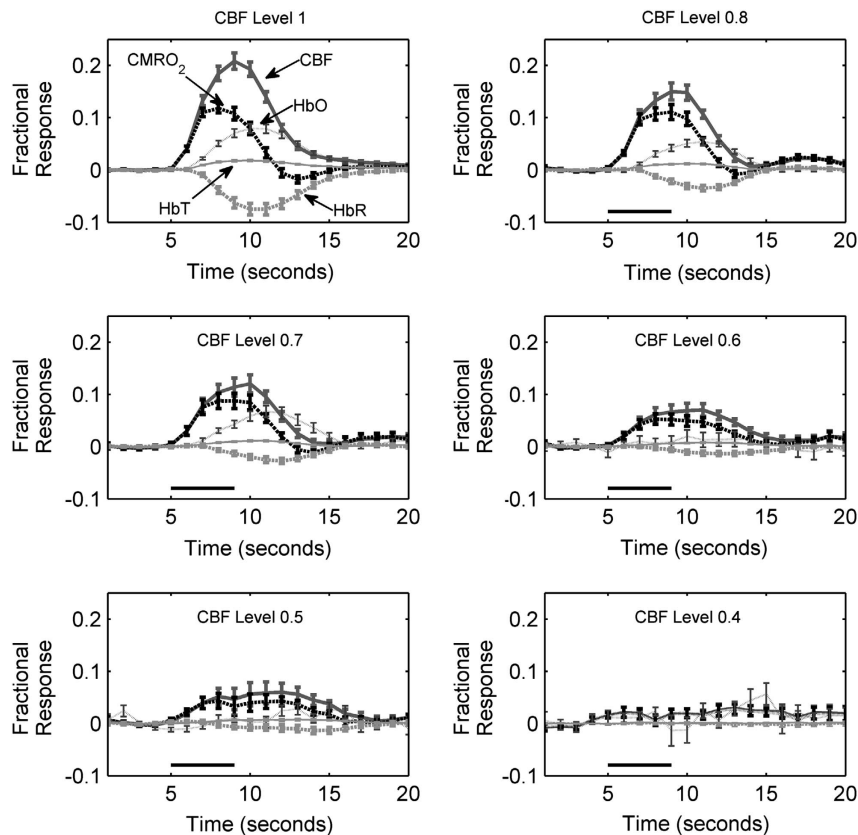


**Figure 4.** The average fractional responses of cerebral blood flow (CBF), cerebral metabolic consumption of oxygen (CMRO<sub>2</sub>), cerebral oxy-hemoglobin (HbO), cerebral deoxy-hemoglobin (HbR), and cerebral total hemoglobin (HbT) measured at various CBF levels (see Equation 3) within the specified bins. The CBF bins are labeled by their central numbers (e.g., CBF Level 0.8 spans the range of CBF levels from 0.75 to 0.85), and the CBF Level 1 indicates the preischemic responses. Here, the CBF bin 0.9 is omitted since the temporal plots look very similar to the preischemic responses. The error bars indicate the standard errors of these averages, and the 4-second forepaw stimulus is indicated in the panels by a thick black line (omitted from CBF Level 1 panel for readability).

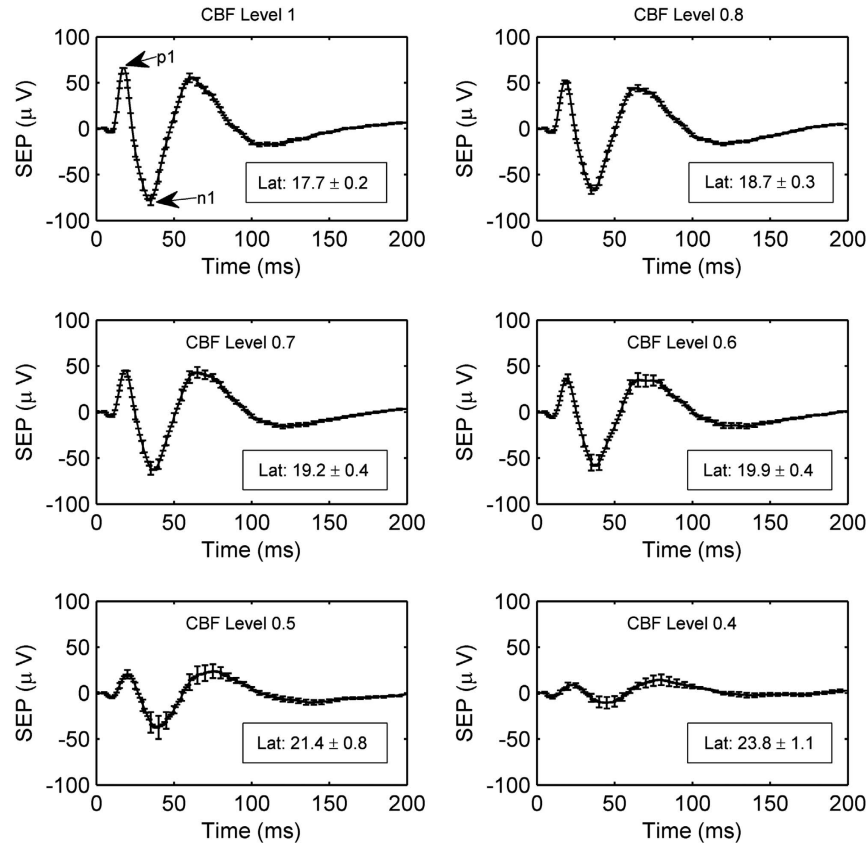


**Figure 5.** The average somatosensory evoked potential (SEP) across animals at each cerebral blood flow (CBF) level bin. As in Figure 4, the CBF level bins are specified by their central numbers. The error bars indicate the standard errors of these averages, and the time zero here corresponds to the arrival of a stimulation pulse. The boxes in each panel contain the SEP latencies (mean  $\pm$  standard error) in milliseconds at each CBF level. The latency is the time from stimulus to the p1 peak. SEP latencies are significantly associated with CBF level ( $P < 0.0001$ ).

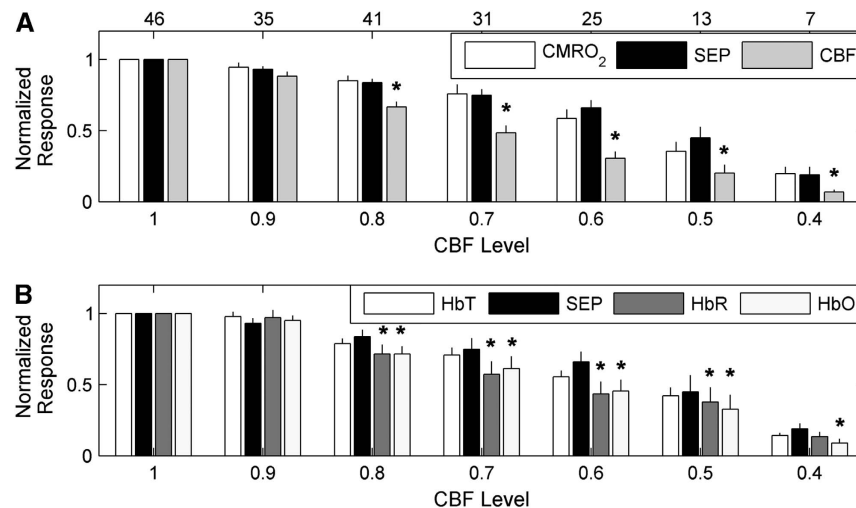


**Figure 6.** Average normalized peak hemodynamic and somatosensory evoked potential (SEP) responses (Equations 2a and 2b) across animals at the binned cerebral blood flow (CBF) levels of ischemia (Equation 3) specified on the horizontal axis. As in Figures 4 and 5, the levels of ischemia are discretized into bins with widths of 10 percentage points, such that a CBF level of 0.9 corresponds to the range of CBF levels between 0.85 and 0.95, a CBF level of 0.8 corresponds to the range of CBF levels between 0.75 and 0.85, etc. **(A)** From left to right, the average normalized cerebral metabolic consumption of oxygen (CMRO<sub>2</sub>), SEP, and CBF responses. **(B)** From left to right, the average normalized cerebral total hemoglobin (HbT), SEP, cerebral oxy-hemoglobin (HbO), and cerebral deoxy-hemoglobin (HbR) responses. The top row of numbers in **(A)** indicates the number of animals contributing to the averages for each CBF level. In both panels, the thin black lines are standard errors to the averages, and the asterisks (\*) denote statistically significant differences ( $P < 0.05$ ) with SEP at a given bin, as determined from a mixed effects model of the mean logarithm of the ratio of SEP with the respective hemodynamic parameter (see Statistical analysis). Recall that by definition, the preischemic response at CBF Level 1 is 1, which is why there are no error bars in the first bins of both panels.

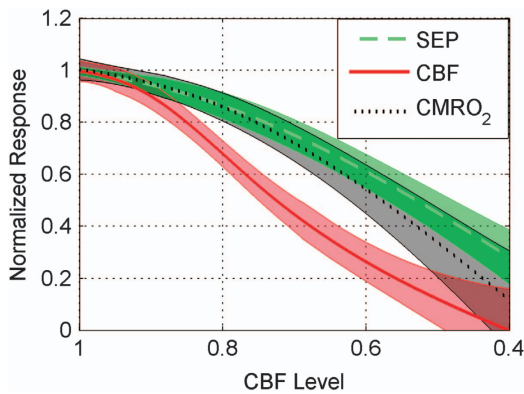


**Figure 7.** Mean normalized response (Equations 2a and 2b) across animals (thick lines) of somatosensory evoked potential (SEP), cerebral blood flow (CBF), and cerebral metabolic consumption of oxygen (CMRO<sub>2</sub>) as a function of CBF level (Equation 3). Mean values shown are based on individual mixed effects models (see Statistical analysis) along with their 95% confidence intervals (shaded regions). CBF differed from SEP ( $P < 0.0001$ ) and CMRO<sub>2</sub> ( $P < 0.0001$ ), but SEP and CMRO<sub>2</sub> were not significantly different ( $P > 0.1$ ).

become more ischemic, whereas the CBF response exhibits a greater attenuation than does SEP. This behavior is confirmed in Figure 7, where instead of discretizing the data into bins, a mixed effects model was used to model averages of CBF, CMRO<sub>2</sub>, and SEP responses at each CBF level. This analysis shows strong evidence of differences among these three response types over the CBF level ( $P < 0.0001$ ) as well as evidence that CBF response differs from SEP ( $P < 0.0001$ ) and from CMRO<sub>2</sub> ( $P < 0.0001$ ). However, there was no significant difference between SEP and CMRO<sub>2</sub> ( $P > 0.1$ ). The mixed effects model analysis comparing SEP with the hemoglobin concentrations HbO, HbR, and HbT also provides strong evidence of differences among these four response types over CBF level ( $P < 0.0001$ ). As with CMRO<sub>2</sub>, there was no significant difference between HbT and SEP, but the SEP response did significantly differ from HbO ( $P < 0.0001$ ) and HbR ( $P < 0.02$ ).

We took the logarithms of the ratios of the SEP response with the three hemodynamic responses (CBF, HbO, and HbR) that differed from SEP over CBF level, and applied individual mixed effects models to them to determine the range of CBF levels where their means are different from zero ( $P < 0.05$ ). These models predict the mean CBF, HbO, and HbR responses first become different from SEP at CBF levels of 0.86, 0.83, and 0.84, respectively. The mean CBF and HbO responses remain different from SEP at all lower CBF levels in the data set, while the mean HbR response is different from SEP until the CBF level of 0.42.

We also note here that in the control group of animals, where no occlusions were made or negative pressure applied, the average normalized hemodynamic and SEP responses across animals did not significantly change (i.e., fluctuations  $< 5\%$ ) over the 2-hour time course of data collection (data not shown).

## DISCUSSION

Fox and Raichle<sup>10</sup> first reported that for healthy humans, the localized CBF increases caused by functional stimulation vastly exceed the localized CMRO<sub>2</sub> increases, although they were comparable to the increases in localized cerebral glucose metabolism.<sup>25</sup> Buxton and Frank<sup>26</sup> explained this observation by developing a compartment model of hemodynamic changes predicting that disproportionately large CBF increases are needed to support small CMRO<sub>2</sub> increases. A key assumption of their

model is that all of the oxygen leaving the vasculature is metabolized, and one consequence of their model is that changes in CBF and CMRO<sub>2</sub> are not independent. However, the direct measurements of tissue oxygen pressure and CBF in rats during functional stimulation, by Ances *et al.*,<sup>21</sup> provide evidence of CBF and CMRO<sub>2</sub> independence, i.e., after 1 minute of stimulation, there was a sustained poststimulus undershoot in tissue oxygen pressure that was not present in CBF. This behavior is similar to the resetting of blood flow and metabolism seen after a more generalized activation (sheltering a rat previously exposed to the environment).<sup>27</sup> Leithner *et al.*<sup>11</sup> also recently presented data in rats showing that the large CBF response from functional stimulation is not necessary to support small changes in CMRO<sub>2</sub>; their interpretation of these results is that a safety factor exists wherein the blood flow increase from functional stimulation can deliver more oxygen than is necessary to sustain the increase in neuronal activity.

Our results show an uncoupling between CBF and CMRO<sub>2</sub> during functional stimulation at different levels of ischemia that supports the notion of the safety factor described by Leithner *et al.*<sup>11</sup> As seen in Figures 6A and 7, the attenuation in functional CBF increases at milder levels of ischemia is stronger than the attenuation in the neuronal activity as measured by SEPs. However, the CMRO<sub>2</sub> response does not follow the CBF response at the milder levels of ischemia, but instead remains coupled to SEP. In other words, the effect of global ischemia is to make the safety factor between the increases in oxygen supply and consumption during functional stimulation smaller.

As with CBF, HbO and HbR are also more severely attenuated with moderate ischemia than the electrical SEP response. However, ischemia does not affect the total hemoglobin response significantly differently from the SEP response (Figure 6B). The uncoupling between blood flow and total hemoglobin responses with ischemia shows that with functional activation, using total hemoglobin as a surrogate for blood flow via Grubb's relation<sup>28</sup> could lead to inaccurate results for blood flow.

Though we are not aware of previously published data on functional hemodynamic responses to an identical stimulation protocol, the preischemic responses we measure are reasonable. For 4 Hz, 4-second, 1.6 mA forepaw stimulation in healthy rats, Royle *et al.*<sup>29</sup> observed an average peak CBF increase of roughly 17% with laser speckle imaging, while Durduran *et al.*<sup>16</sup> observed average peak CBF increases with laser speckle imaging of  $13.4 \pm 2.5\%$  and  $20.0 \pm 3.0\%$  for 5 Hz, 4-second stimulations with amplitudes of 1 and 2 mA, respectively. Furthermore, the ratios between the average peak CBF response and the average peak CMRO<sub>2</sub>, HbO, HbR, and HbT responses in our preischemic data are comparable to functional responses reported by Dunn *et al.*<sup>17</sup> The small poststimulus undershoot in CMRO<sub>2</sub> shown in Figure 4, as well as the simultaneous rise of CBF and CMRO<sub>2</sub>, is likely an artifact of the steady-state model, Equation 1.<sup>30</sup>

In regard to SEPs, experimental work involving a focal ischemia model in baboons showed a sharp CBF threshold for electrical activity in the brain, with complete electrical failure when CBF is  $\sim 35\%$  of control.<sup>31</sup> A similar CBF threshold was observed for auditory evoked potentials in a global ischemia model in cats.<sup>32</sup> In our study, we did observe severe attenuation in SEPs at a CBF level around 40% (Figures 5–7), although we did not observe the same sharp CBF threshold for electrical activity seen in these nonrodent ischemia models (Figure 7). There is a scarcity of data examining SEPs at milder levels of ischemia. One paper examining SEPs in a hemorrhage ischemia rat model observed SEP amplitudes between 50% and 60% of control when CBF was decreased to  $\sim 65\%$  of control,<sup>33</sup> which is reasonably close to the results in Figure 7. In another paper examining the effects of bilateral common carotid artery occlusion on SEPs in rats, a steady-state decrease in the SEP p1 amplitude to 90% of control is observed, although this decrease was not statistically significant.<sup>34</sup> In the

present study, bilateral common carotid artery occlusion decreased CBF to  $70 \pm 15\%$  (mean  $\pm$  SD) of control. Since in the control group, the SEP amplitude remains stable, it is likely that the observed decreases in SEP amplitude during mild ischemia are in fact because of the reduced blood flow levels in the brain. The effect of an increased SEP latency with ischemia (Figure 5) has been observed in rodent models of ischemia by others as well.<sup>35,36</sup>

The mechanisms that couple changes in neuronal activity to changes in CBF have been under investigation for several decades and involve not only the neurons but also the vascular cells and astrocytes encompassing the 'so-called' neurovascular unit.<sup>37</sup> The main mediators for the hemodynamic response to neuronal activation include nitric oxide, adenosine, glutamate, arachidonic acid metabolites, and epoxyeicosatrienoic acids.<sup>2</sup> During and after cerebral ischemia, the elements that comprise the neurovascular unit may be altered and vascular reactivity depressed,<sup>38</sup> with the degree of depression dependent on the degree of ischemia.<sup>39</sup> However, data are lacking on changes to these mediators during graded ischemia. Although a specific mechanism accounting for the decrease in blood flow response as baseline blood flow decreased cannot be identified, reduction of CBF resulting from upstream vascular clamping or hypotension causes the local vasculature to dilate with potential negative implications for further dilation in response to neuronal activation. It is also important to note that *global* ischemia, which was used in the present study, could have different effects on the neurovascular unit compared with *focal* ischemia. For example, during focal ischemia functional stimulation may have the potential for activation of collateral blood flow through leptomeningeal anastomoses.

To summarize, we have collected a large data set of hemodynamic and electrical functional responses in rats at many different levels of global cerebral ischemia. All of the electrical and hemodynamic responses are attenuated as the global ischemia becomes more severe, but the blood flow, oxy-hemoglobin, and deoxy-hemoglobin responses are more strongly attenuated at milder levels of global ischemia than the electrical or metabolic responses. The observed uncoupling between flow and metabolism at ischemic levels is evidence supporting the notion that during healthy conditions, functional stimulation increases oxygen delivery to brain tissue more than oxygen consumption. During functional stimulation in global ischemia, though, a higher fraction of the oxygen delivered from the vasculature will be consumed.

## DISCLOSURE/CONFLICT OF INTEREST

The authors declare no conflict of interest.

## ACKNOWLEDGEMENTS

The content is solely the responsibility of the authors and does not necessarily represent the official views of the Eunice Kennedy Shriver National Institute of Child Health and Human Development or the National Institutes of Health. The authors are also grateful to Chao Zhou and Eric Pinter for their assistance with building the optical imaging instrument.

## REFERENCES

- Vanzetta I, Grinvald A. Coupling between neuronal activity and microcirculation: implications for functional brain imaging. *HFSP J* 2008; **2**: 79–98.
- Iadecola C. Neurovascular regulation in the normal brain and in Alzheimer's disease. *Nat Rev Neurosci* 2004; **5**: 347–360.
- del Zoppo GJ. The neurovascular unit in the setting of stroke. *J Intern Med* 2010; **267**: 156–171.
- Boas DA, Dunn AK. Laser speckle contrast imaging in biomedical optics. *J Biomed Opt* 2010; **15**: 011109.
- Dunn AK, Bolay T, Moskowitz MA, Boas DA. Dynamic imaging of cerebral blood flow using laser speckle. *J Cereb Blood Flow Metab* 2001; **21**: 195–201.
- Dunn AK, Devor A, Hayrunnisa B, Andermann ML, Moskowitz MA, Dale AM et al. Simultaneous imaging of total cerebral hemoglobin, oxygenation, and blood flow during functional activation. *Opt Lett* 2003; **28**: 28–30.
- Grinvald A, Lieke E, Frostig RD, Gilbert CD, Wiesel TN. Functional architecture of cortex revealed by optical imaging of intrinsic signals. *Nature* 1986; **272**: 361–364.
- Burnett MG, Shimazu T, Szabados T, Muramatsu H, Detre JA, Greenberg JH. Electrical forepaw stimulation during reversible forebrain ischemia decreases infarct volume. *Stroke* 2006; **37**: 1327–1331.
- Lay CC, Davis MF, Chen-Bee CH, Frostig RD. Mild sensory stimulation completely protects the adult rodent cortex from ischemic stroke. *PLoS ONE* 2010; **5**: e11270.
- Fox PT, Raichle ME. Focal physiological uncoupling of cerebral blood flow and oxidative metabolism during somatosensory stimulation in human subjects. *Proc Natl Acad Sci USA* 1986; **83**: 1140–1144.
- Leithner C, Royl G, Offenhauser N, Fuchtemeier M, Kohl-Bareis M, Villringer A et al. Pharmacological uncoupling of activation induced increases in CBF and CMRO<sub>2</sub>. *J Cereb Blood Flow Metab* 2010; **30**: 311–322.
- Vazquez AL, Masamoto K, Kim SG. Dynamics of oxygen delivery and consumption during evoked neural stimulation using a compartment model and CBF and tissue P(O<sub>2</sub>) measurements. *Neuroimage* 2008; **42**: 49–59.
- Dirnagl U, Thorén P, Villringer A, Sixt G, Them A, Einhüpl KM. Global forebrain ischaemia in the rat: controlled reduction of cerebral blood flow by hypobaric hypotension and two-vessel occlusion. *Neuro Res* 1993; **15**: 128–130.
- Zhou C, Shimazu T, Durduran T, Luckl J, Kimberg DY, Yu G et al. Acute functional recovery of cerebral blood flow after forebrain ischemia in rat. *J Cereb Blood Flow Metab* 2008; **28**: 1275–1284.
- Parthasarathy AB, Kazmi SM, Dunn AK. Quantitative imaging of ischemic stroke through thinned skull in mice with multi exposure speckle imaging. *Biomed Opt Express* 2010; **1**: 246–259.
- Durduran T, Burnett MG, Yu G, Zhou C, Furuya D, Yodh AG et al. Spatiotemporal quantification of cerebral blood flow during functional activation in rat somatosensory cortex using laser-speckle flowmetry. *J Cereb Blood Flow Metab* 2004; **24**: 518–525.
- Dunn AK, Devor A, Dale AM, Boas DA. Spatial extent of oxygen metabolism and hemodynamic changes. *Neuroimage* 2005; **27**: 279–290.
- Kohl M, Lindauer U, Royl G, Kuhl M, Gold L, Villringer A et al. Physical model for the spectroscopic analysis of cortical intrinsic optical signals. *Phys Med Biol* 2000; **45**: 3749–3764.
- Culver JP, Durduran T, Furuya D, Cheung C, Greenberg JH, Yodh AG. Diffuse optical tomography of cerebral blood flow, oxygenation, and metabolism in rat during focal ischemia. *J Cereb Blood Flow Metab* 2003; **23**: 911–924.
- Yaseen MA, Srinivasan VJ, Sakadzic S, Radhakrishnan H, Gorczynska I, Wu W et al. Microvascular oxygen tension and flow measurements in rodent cerebral cortex during baseline conditions and functional activation. *J Cereb Blood Flow Metab* 2011; **31**: 1051–1063.
- Ances BM, Buerk DG, Greenberg JH, Detre JA. Temporal dynamics of the partial pressure of brain tissue oxygen during functional forepaw stimulation in rats. *Neurosci Lett* 2001; **306**: 106–110.
- Jones M, Berwick J, Johnston D, Mayhew J. Concurrent optical imaging spectroscopy and laser-doppler flowmetry: the relationship between blood flow, oxygenation, and volume in rodent barrel cortex. *Neuroimage* 2001; **13**: 1002–1015.
- Pinheiro JC, Bates DM. *Mixed-Effects Models in S and S-plus*. Springer: New York, NY, 2000.
- R Foundation for Statistical Computing 2011R: *A Language and Environment for Statistical Computing* <http://www.R-project.org>.
- Fox PT, Raichle ME, Mintun MA, Dence C. Nonoxidative glucose consumption during focal physiologic neural activity. *Science* 1988; **241**: 462–464.
- Buxton RD, Frank LR. A model for the coupling between cerebral blood flow and oxygen metabolism during neural stimulation. *J Cereb Blood Flow Metab* 1997; **17**: 64–72.
- Madsen PL, Linde R, Hasselbalch SG, Paulson OB, Lassen NA. Activation-induced resetting of cerebral oxygen and glucose uptake in the rat. *J Cereb Blood Flow Metab* 1998; **18**: 742–748.
- Grubb Jr RL, Raichle ME, Eichling JO, Ter-Pogossian MM. The effects of changes in PaCO<sub>2</sub> on cerebral blood volume, blood flow, and vascular mean transit time. *Stroke* 1974; **5**: 630–639.
- Royl G, Leithner C, Selliena H, Müller JP, Megowa D, Offenhauser N et al. Functional imaging with Laser Speckle Contrast Analysis: vascular compartment analysis and correlation with Laser Doppler Flowmetry and somatosensory evoked potentials. *Brain Res* 2006; **1121**: 95–103.
- Vazquez AL, Fukuda M, Kim SG. Evolution of the dynamic changes in functional cerebral oxidative metabolism from tissue mitochondria to blood oxygen. *J Cereb Blood Flow Metab* 2012; **32**: 745–758.
- Branston NM, Symon L, Crockard HA, Pasztor E. Relationship between the cortical evoked potential and local cortical blood flow following acute middle cerebral artery occlusion in the baboon. *Exp Neurol* 1974; **45**: 195–208.
- Shimada N, Graf R, Rosner G, Heiss WD. Differences in ischemia-induced accumulation of amino acids in the cat cortex. *Stroke* 1990; **21**: 1445–1551.

- 33 Skarphedinsson JO, Delle M, Carlsson S, Bealer SL. The effects of hexamethonium on cerebral blood flow and cerebral function during relative cerebral ischaemia in rats. *Acta Physiol Scand* 1996; **158**: 21–28.
- 34 Block F, Sontag KH. Differential effects of transient occlusion of common carotid arteries in normotensive rats on the somatosensory and visual system. *Brain Res Bull* 1994; **33**: 589–593.
- 35 Henninger N, Heimann A, Kempfski O. Electrophysiology and neuronal integrity following systemic arterial hypotension in a rat model of unilateral carotid artery occlusion. *Brain Res* 2007; **1163**: 119–129.
- 36 Wang Y, Shiraiishi Y, Kawai Y, Nakashima K. Ligation of lateral carotid artery attenuates disturbance of brain function caused by subsequent cerebral ischemia in rabbits. *Neurosci Lett* 1996; **218**: 119–122.

- 37 Lecrux C, Hamel E. The neurovascular unit in brain function and disease. *Acta Physiol* 2011; **203**: 47–59.
- 38 Clavier N, Kirsch JR, Hurn PD, Traystman RJ. Effect of postischemic hypoperfusion on vasodilatory mechanisms in cats. *Am J Physiol* 1994; **267**: H2012–H2018.
- 39 Jones SC, Bose B, Furlan AJ, Friel HT, Easley KA, Meredith MP *et al*. CO<sub>2</sub> reactivity and heterogeneity of cerebral blood flow in ischemic, border zone, and normal cortex. *Am J Physiol* 1989; **257**: H473–H482.
- 40 Jones PB, Shin HK, Boas DA, Hyman BT, Moskowitz MA, Ayata C *et al*. Simultaneous multispectral reflectance imaging and laser speckle flowmetry of cerebral blood flow and oxygen metabolism in focal cerebral ischemia. *J Biomed Opt* 2008; **13**: 044007.

## APPENDIX

A modified Beer–Lambert law was used to compute oxy-hemoglobin concentration (HbO) and deoxy-hemoglobin concentration (HbR) changes from intensity measurements under light emitting diode (LED) illumination:

$$\log_{10} \frac{I_{jk}(t)}{I_{0,jk}} = \sum_i w_i \{ \epsilon_{HbO}(\lambda_i) \Delta HbO_k(t) + \epsilon_{HbR}(\lambda_i) \Delta HbR_k(t) \} D(\lambda_i) \quad (A1)$$

Here,  $I_{jk}(t)$  is the measured intensity at time  $t$  and  $I_{0,jk}$  is the averaged measured prestimulus baseline intensity at a given ischemic condition for LED  $j$  and pixel  $k$  in the CCD camera,  $\epsilon_{HbO}(\lambda)$  and  $\epsilon_{HbR}(\lambda)$  are molar extinction coefficients for HbO and HbR at wavelength  $\lambda$ , respectively,  $\Delta HbO_k(t)$  and  $\Delta HbR_k(t)$  are the concentration changes in HbO and HbR from baseline at pixel  $k$  and time  $t$ , respectively,  $D$  is a differential pathlength,  $w_i$  are weights indicating the contribution of wavelength  $\lambda_i$  in the spectra of LED  $j$ , and the sum is over all  $i$  wavelengths present in the LED spectra. Equation A1 assumes that light absorption from tissue chromophores other than HbO and HbR is negligible, and that tissue scattering remains constant over time. The LEDs had a broad spectra (width > 20 nm), which is why it was necessary to measure the emission spectra of the three LEDs used with a spectrophotometer.

The weight  $w_i$  in Equation A1 is the power of wavelength  $\lambda_i$  emitted by a given LED divided by the total power emitted by the LED over all wavelengths. Using Monte Carlo simulations, the differential pathlengths at each wavelength in the LED spectra were calculated with the procedure described by Kohl *et al*.<sup>18</sup> The mean differential pathlengths for the 530, 590, and 660 nm LEDs

we used were 0.063, 0.087, and 0.474 cm, respectively. Equation 1 forms a system of three equations for each of the three LEDs, which was solved for  $\Delta HbO_k(t)$  and  $\Delta HbR_k(t)$  using a least squares approach.

In addition to using Equation A1 to calculate changes in HbO and HbR because of stimulation at a given ischemic condition, Equation A1 was also used to calculate changes in HbO and HbR between adjacent steps of graded ischemia. For example, to measure the changes in HbO and HbR because of right carotid artery occlusion,  $I_{jk}$  and  $I_{0,jk}$  in the left-hand side of Equation A1 are the average prestimulus intensities during the right carotid artery occlusion and the preischemic baseline periods, respectively, for LED  $j$  and pixel  $k$  (Figure 2). HbO and HbR changes between right carotid artery occlusion and bilateral carotid artery occlusion, bilateral carotid artery occlusion and three vessel occlusion, and three vessel occlusion and negative lower body pressure were calculated in the same way. The changes in HbO and HbR between adjacent steps of graded ischemia are small enough that the modified Beer–Lambert Law (Equation A1) is still accurate.<sup>40</sup>

It was assumed during the preischemic baseline period for every animal that the cortical tissue under the imaging window is spatially homogeneous with  $HbO_0 = 60 \mu\text{mol/L}$ ,  $HbR_0 = 40 \mu\text{mol/L}$ , and a reduced scattering coefficient of 10 per cm for all wavelengths emitted by the LEDs. From this starting point, images of HbO and HbR were then calculated for all subsequent conditions of ischemia. These measurements of hemoglobin concentration ( $\mu\text{mol}/\text{volume tissue}$ ) are averaged over a well-mixed sample of arterioles, capillaries, and venules.